COMPRESSIVE SENSING WITH AN OVERCOMPLETE DICTIONARY FOR HIGH-RESOLUTION DFT ANALYSIS

Guglielmo Frigo and Claudio Narduzzi

University of Padua
Department of Information Engineering – DEI
via G. Gradenigo 6/b, I–35131 Padova, Italy

ABSTRACT

The problem of resolving frequency components close to the Rayleigh threshold, while using time-domain sample sequences of length not greater than N, is relevant to several waveform monitoring applications where acquisition time is upper-bounded. The paper presents a compressive sensing (CS) algorithm that enhances frequency resolution by introducing a dictionary that explicitly accounts for spectral leakage on a fine frequency grid. The proposed algorithm achieves good estimation accuracy without significantly extending total measurement time.

Index Terms— discrete Fourier transform, spectral analysis, compressive sensing, super-resolution

1. INTRODUCTION

Frequency-domain waveform analysis is a problem for which a variety of well-known solutions have been proposed in the literature [1], [2]. A multisine waveform can be expressed as a sum of cisoids, whose spectrum after sampling is a complex-weighted spike train:

$$X(\lambda) = \sum_h A_h e^{j\phi_h} \delta(\lambda - \lambda_h). \qquad (1)$$

Here, as in the following, frequency $\lambda \in [0, 1]$ is normalized with respect to the sampling rate $f_s = \frac{1}{T_s}$ (i.e., $\lambda = f T_s$).

Non-parametric approaches based on the discrete Fourier transform have been a workhorse of waveform analysis for decades [3]. Given a sample sequence of length N, its discrete Fourier transform (DFT) coefficients are located on a frequency grid with step $\Delta_\lambda = \frac{1}{N}$. Therefore, they represent (1) exactly only when spike locations λ_h fall on this grid.

Reconstruction by DFT alone yields poor results for off-grid frequencies, as the capability to resolve signal components at closely spaced frequencies is limited by spectral leakage. Interpolation of DFT coefficients [4] can provide much more accurate estimates of the weights $A_h e^{j\phi_h}$ and the off-grid normalized frequencies λ_h, with variances approaching the relevant Cramér-Rao bounds [5]. However, required minimum separation between adjacent frequencies is increased by

a factor k_R, that depends on the kind of interpolation algorithm and on the weighting (if any) applied to the time-domain samples.

Since $k_R > 1$, the minimum allowed distance $k_R \Delta_\lambda$ is always significantly larger than Δ_λ. Parametric approaches, e.g., Pisarenko harmonic decomposition, MUSIC and ESPRIT, can allow much better resolution, but do so at the price of greater computational complexity.

In this paper the problem is addressed by introducing a finer frequency grid, with smaller step size Δ'_λ, and relating the set of N samples to $N' = P \cdot N$ coefficients of the DFT defined on the finer grid, that is associated to an integer super-resolution or *refinement* factor $P = \frac{\Delta_\lambda}{\Delta'_\lambda}$.

In the literature on compressive sensing (CS), super-resolution algorithms based on this idea have been proposed. Random waveform samples can be related to DFT coefficients by way of the measurement equation:

$$\mathbf{x} = \mathbf{W}^H_{(N \times N')} \, \mathbf{a} + \mathbf{z}, \qquad (2)$$

where $\mathbf{x} \in \mathbb{R}^N$ contains N time-domain samples $x(n)$ and elements of $\mathbf{a} \in \mathbb{C}^{N'}$ are DFT coefficients on the finer grid. Vector $\mathbf{z}$ represents additive zero-mean white noise with variance σ_z^2. In the standard approach $\mathbf{W}^H_{(N \times N')}$ is a compressive random measurement matrix defined as a $N \times N'$ partial inverse Fourier transform, whose rows are randomly drawn from the full $N' \times N'$ matrix. A fine-grid solution can be found by convex ℓ^1 minimization, exploiting an *a-priori* sparsity constraint on vector $\mathbf{a}$, provided a minimum distance $4\Delta_\lambda$ exists between adjacent components [6], [7]. The issue of poor numerical conditioning caused by highly coherent column vectors in $\mathbf{W}^H_{(N \times N')}$ is addressed by algorithms based on *frequency inhibition* [8] or coherence *band exclusion* [9], the latter achieving a minimum separation of $3\Delta_\lambda$. Components whose frequency separation is closer to the Rayleigh threshold Δ_λ seemingly remain unresolvable by CS methods.

We show in this paper that a CS approach can indeed resolve closely spaced frequency components, when $\mathbf{x}$ contains *sequentially* sampled values, if the measurement equation is suitably defined to reflect this. Rather than adapt matrix $\mathbf{W}^H_{(N \times N')}$, as in [10], we exploit the feature by explicitly

introducing information about spectral leakage into the measurement equation. With our approach this becomes:

$$\mathbf{x} = \mathbf{W}^H \mathbf{D} \mathbf{a} + \mathbf{z}, \tag{3}$$

where $\mathbf{W}^H$ is a full inverse DFT of smaller size $N \times N$ and spectral leakage is modelled by matrix $\mathbf{D}$, of size $N \times N'$. The latter is in fact an overcomplete convolutional dictionary [11], whose structure is presented in the next Section.

In the following, we discuss and characterize the proposed CS-based high-resolution DFT analysis, proving by numerical simulation that components as close as $1.5\Delta_\lambda$ can be successfully resolved. As a further advantage, total acquisition time for $\mathbf{x}$ in (3) is strictly NT_S, whereas random sampling acquisition of $\mathbf{x}$ in (2) approximately requires the time $N'T_S$.

The improved lower bound on frequency separation is of interest in monitoring applications, where it reduces the need to acquire longer sample sequences for a given resolution, thereby avoiding possible adverse effects on the capability to track waveform variations.

2. DICTIONARY-BASED MEASUREMENT EQUATION

The N-sample DFT of a waveform whose spectrum is given by (1) is:

$$\tilde{X}\left(\frac{k}{N}\right) = \sum_h A_h e^{j\phi_h} D_N\left(\frac{k}{N} - \lambda_h\right) e^{-j2\pi\left(\frac{k}{N} - \lambda_h\right)n_0} \tag{4}$$

with $0 \le k < N$. The integer n_0 is the index of the start sample in the acquired sequence and $D_N(\cdot)$ is the Dirichlet kernel:

$$D_N(\lambda) = \frac{\sin \pi N\lambda}{N \sin \pi\lambda} e^{-j\pi(N-1)\lambda} \tag{5}$$

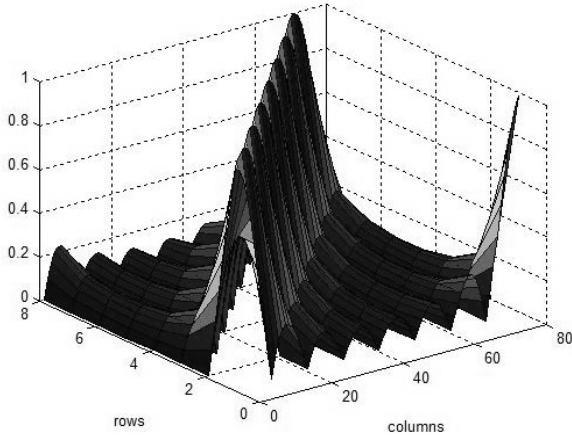which accounts for the leakage effect due to the finite sequence length N.

Fig. 1. Three-dimensional representation of matrix $\mathbf{D}$ [18].

Table 1. Minimum distance – equal-amplitude components.

P	3	5	7	9	11	13
Δl	5	8	10	13	16	22
$\|\lambda_2 - \lambda_1\| \cdot N$	**1.67**	**1.6**	**1.43**	**1.44**	**1.45**	**1.69**
P	15	17	19	21	23	
Δl	22	26	28	30	34	
$\|\lambda_2 - \lambda_1\| \cdot N$	**1.47**	**1.53**	**1.47**	**1.43**	**1.48**	

DFT coefficients are in fact samples of the frequency-domain convolution: $X(\lambda) * D_N(\lambda)$, where the Dirichlet kernel plays the role of a *resolution* or *point spread* function with respect to the signal spectrum. Considering a finer frequency grid with step size Δ'_λ, without changing N, is equivalent to sampling the same function at more closely spaced intervals. Measurement equation (3) accounts for this by explicitly introducing matrix $\mathbf{D}$, with elements: $d_{k,l} = D_N\left(\frac{k}{N} - \frac{l}{N'}\right)$, that represents spectral leakage through values of the Dirichlet kernel computed on a two-dimensional grid. The structure of this matrix is graphically presented in Fig. 1.

CS algorithms look for the sparsest solution of (3). The vector $\mathbf{a}$ having the minimum number of non-zero elements (i.e., minimum pseudo-norm $\|\mathbf{a}\|_0$) can be obtained either by solving a constrained ℓ^1 problem, or by a greedy algorithm. Taking the latter alternative, we use orthogonal matching pursuit (OMP) [12] to recover the *support* of $\mathbf{a}$, that is, the set S_a of indices associated to non-zero vector elements a_l. Formally: $S_a = \{l : |a_l| \ne 0, l \in [0, 1, \dots, N'-1]\}$.

Fine-grid DFT coefficients are the non-zero elements of $\mathbf{a}$, whose values are determined by computing the pseudo-inverse:

$$\hat{\mathbf{a}}_S = \frac{1}{N}\left(\mathbf{D}_S^H \mathbf{D}_S\right)^{-1} \mathbf{D}_S^H \mathbf{W} \mathbf{x}. \tag{6}$$

In this equation, $\mathbf{D}_S$ is a *restricted* dictionary matrix obtained by keeping only the columns of $\mathbf{D}$ with index $l \in S_a$, and $\hat{\mathbf{a}}_S$ is the correspondingly restricted vector.

Support recovery is the critical part of the algorithm, as its task is to identify waveform components. Its function is the equivalent, on the finer frequency grid, of peak search in traditional DFT-based spectral analysis and, likewise, a signal-to-noise ratio (SNR) threshold holds.

To find out the lower bound for frequency separation we considered a signal with $|S_a| = 3$, i.e., three cisoidal components, each having unit amplitude and initial phase randomly taken from a uniform distribution between 0 and 2π. In the frequency domain two components, at frequencies λ_1 and λ_2, had their distance progressively reduced, while the third, located further away, was employed as a control element.

The limiting distance between the two close components was determined when support recovery success rate dropped below 100%. Results obtained in noiseless conditions are reported in Table 1, where Δl is the minimum difference between the indexes of the corresponding two non-zero vector

elements a_{l_1} and a_{l_2}, and $|\lambda_2 - \lambda_1| \cdot N = \frac{\Delta l}{P}$.

Considering a sequence length $N = 256$, trials were repeated for different super-resolution factors. We assigned to P integer values between 3 and 23 (a range of non-critical values for the numerical conditioning of $\mathbf{D}$), selecting only coprimes with N to prevent $\mathbf{D}$ from becoming singular. Fine grid step size is thus approximately one order of magnitude smaller than Δ_λ. Within the given range for P the threshold lies at approximately $1.5\Delta_\lambda$, that is, half the value required by coherence band exclusion [9]. Variability in the computed value of $\Delta_\lambda \cdot N$ is due to the fact that only frequencies falling exactly on the finer grid have been considered, to avoid interaction with finite-grid errors that are the object of separate tests discussed in the next Section.

Results obtained for different values of the signal-to-noise ratio (SNR) show that, for a sequence of $N = 256$ samples, S_a is correctly recovered down to approximately SNR = 15 dB. This means 100% success rate in finding components whose frequencies λ_h lie on the finer grid.

Plots of success probability versus SNR, for $N = 256$ and different values of the super-resolution factor P, are presented in Fig. 2. Some performance degradation is apparent as P gets larger, since coherence among the columns of $\mathbf{D}$ is increased as well. Nevertheless, OMP can still achieve a success rate in excess of 90% with SNR = 10 dB and $P < 15$.
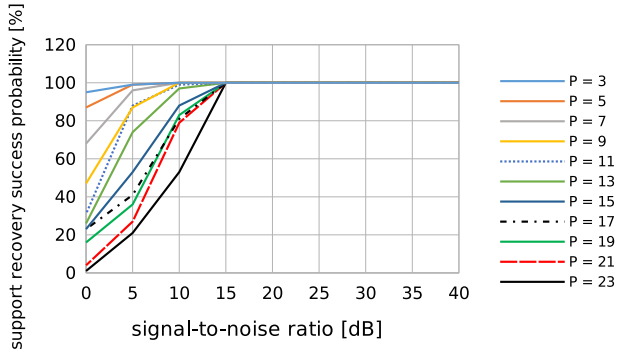

Fig. 2. Probability of successful support recovery for different values of SNR and super-resolution factor P.

3. FINITE-GRID ERROR AND NOISE

Amplitude estimation by (6) can yield accurate estimates, whose covariance with noisy data is:

$$\text{cov}[\hat{\mathbf{a}}_S] = \frac{\sigma_z^2}{N} \left(\mathbf{D}_S^H \mathbf{D}_S \right)^{-1}. \tag{7}$$

Matrix $\mathbf{D}_S^H \mathbf{D}_S$ approximates the identity for component separations greater than Δ_λ, so that amplitude estimates are, for practical purposes, uncorrelated and their variance is close to the single-component Cramèr-Rao bound [14]. This was
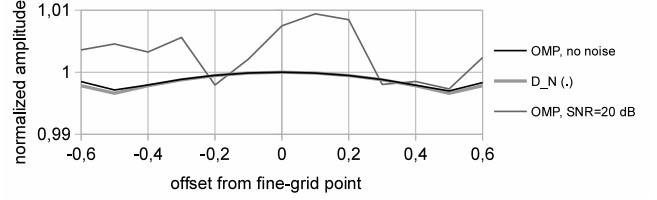

Fig. 3. Amplitude estimation for a single off-grid component.

confirmed by a set of 100 simulations, repeated for different values of SNR, considering again the three-component signal introduced in the previous Section. A super-resolution factor $P = 11$ was selected as it is a prime integer and approximately corresponds to an order-of-magnitude improvement of the frequency grid step size, that is, equivalent to what can safely be achieved in practice by the interpolated DFT approach [4]. The first two waveform components were placed quite close to each other, at $(\lambda_2 - \lambda_1) \cdot N = \frac{14}{11} = 1.27$, while the third, included as a far-distance reference, was at $(\lambda_3 - \lambda_2) \cdot N = \frac{292}{11} = 26.5$. Over a wide range of SNR values, estimated amplitude variances differed very little among them, their values being only marginally larger than the quantity $\frac{\sigma_z^2}{N}$.

Component frequencies may not actually coincide with grid points, therefore to a more limited extent leakage can still be present. To show how amplitude estimates are affected, the plots of Fig. 3 were obtained by varying the frequency of a single sinusoidal component in a $\pm 0.5\Delta_\lambda'$ neighborhood of a fine-grid point $\frac{k_h}{N'}$. In the noiseless case, relative error in amplitude estimation is almost exactly $1 - D_N(\Delta_\lambda')$ and depends on the scalloping loss associated to the Dirichlet kernel [13]. The largest error occurs for $|\lambda| = 0.5\Delta_\lambda'$, but attenuation is much smaller than the Dirichlet kernel worst-case scalloping loss, since $D_N(0.5\Delta_\lambda') \gg D_N(0.5\Delta_\lambda)$ even with the moderate super-resolution factor $P = 11$ employed for the plots.

Fig. 3 also presents an example where signal samples are affected by zero-mean random white noise with SNR = 20 dB. The plot shows that estimate variations caused by noise can be considerably larger than scalloping loss effects. To further analyze the latter aspect, a set of 100 simulations with a single sinusoidal component and SNR = 20 dB was repeated at a number of frequencies within $\pm 0.5\Delta_\lambda'$ of a fine-grid point. In this case the total root-mean-square error is a more useful performance indicator than pure variance, since the resulting mean deviation from reference values is significant. This is plotted in Fig. 4 and, when compared with Fig. 3, shows the considerable impact of noise.

4. SUPPORT RECOVERY FOR LOW SNR

The success rate of the non-linear support recovery stage included in the CS algorithm drops significantly when SNR gets
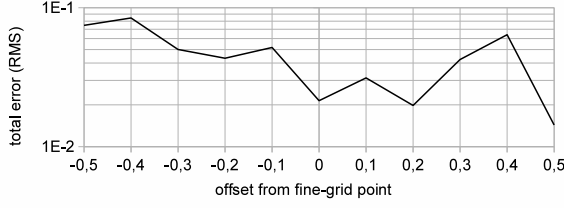
Fig. 4. Total root-mean-square error for amplitude estimation of a single off-grid component, with SNR = 20 dB.

below a certain limiting value, as shown in Fig. 2. This performance can be enhanced, at the cost of a moderate increase in measurement time, by jointly processing a set of time-shifted but strongly overlapped N-sample sequences.

For this purpose we consider a set of M measurement vectors $\mathbf{x}_m$, with $0 \leq m < M$, each containing N sequentially acquired waveform samples. The index of the first sample in each sequence is known, since one may start from 0 for the first acquisition, and simply record the index difference at the start of subsequent records. With this convention, the start index of a sequence will be indicated by n_m and $n_0 = 0$. Setting $\Delta n = n_{m+1} - n_m$, the total acquisition length becomes: $N + (M - 1) \cdot \Delta n$.

To understand the effect of an index shift on the measurement equation, it is useful to consider DFT expression (4). Given a sample record starting at n_m, each complex term in the summation on the right-hand side has the form:

$$A_h e^{j(\phi_h - 2\pi \lambda_h n_m)} D_N\left(\frac{k}{N} - \lambda_h\right) e^{-j2\pi \frac{k}{N} n_m}, \qquad (8)$$

where the exponential term at the end of the expression is independent of the frequency λ_h. This can actually be set to zero assuming that, whenever a DFT is computed, the time index runs from 0 to $N - 1$, rather than from n_m to $n_m + N - 1$.

Each vector $\mathbf{x}_m$ can therefore be associated to a measurement equation of the form (3): $\mathbf{x}_m = \mathbf{W}^H \mathbf{D} \mathbf{a}_m + \mathbf{z}_m$, where vectors $\mathbf{z}_m$ are uncorrelated, being time-shifted with respect to each other. On the other hand, the net effect of an index shift on the waveform-related term is a phase rotation of the complex weight associated to the h-th waveform component, by the quantity $-2\pi \lambda_h n_m$. Neither magnitude A_h nor, more importantly, frequency location λ_h are affected. Consequently, the support set S_a is common to all vectors $\mathbf{a}_m$.

After arranging the set of measurement vectors into an $N \times M$ matrix $\mathbf{X} = [\mathbf{x}_0, \mathbf{x}_1 \ldots, \mathbf{x}_M - 1]$, our problem can be formulated by means of a *multiple measurement vector* (MMV) equation with *jointly sparse* support [15]:

$$\mathbf{X} = \mathbf{W}^H \mathbf{D} \mathbf{A} + \mathbf{Z}, \qquad (9)$$

with $\mathbf{Z} = [\mathbf{z}_0, \mathbf{z}_1 \ldots, \mathbf{z}_M - 1]$. Matrix $\mathbf{A}$, with size $N' \times M$, can be factorized as:

$$\mathbf{A} = \text{diag}\{\mathbf{a}\}\mathbf{R}. \qquad (10)$$

where diag$\{\mathbf{a}\}$ is a diagonal $N' \times N'$ matrix whose non-zero entries are the elements of vector $\mathbf{a}$. The M columns of $\mathbf{R}$ contain the phase rotation terms defined at each point of the fine frequency grid for each time shift n_m.

For the measurement correlation matrix $\mathbf{X}\mathbf{X}^T$ the following equality holds:

$$\mathbf{X}\mathbf{X}^T = \mathbf{W}^H \mathbf{D}\left(\sum_{i=0}^{M-1} \mathbf{a}_i \mathbf{a}_i^H\right)\mathbf{D}^H \mathbf{W} + \sum_{i=0}^{M-1} \mathbf{z}_i \mathbf{z}_i^T \qquad (11)$$

where, as already noted, white noise vectors are uncorrelated. Therefore, we can apply singular-value decomposition (SVD): $\mathbf{X}\mathbf{X}^T = \mathbf{V}_X \cdot \text{diag}[\lambda_i^2] \cdot \mathbf{V}_X^H$, with $\lambda_1 > \lambda_2, \ldots, \lambda_N$ to separate signal and noise subspaces. Since the signal subspace rank is equal to the order of the signal model (1), a condition involving the cardinality of S_a, namely: $M > |S_a|$, must be satisfied, which determines the minimum size of the measurement correlation matrix.

Interpretation of SVD as a Karhunen-Loève expansion for $\mathbf{X}\mathbf{X}^T$ suggests that, by increasing M, at low SNR values the larger eigenvalues will increase their energy without increasing in number, whereas noise-related eigenvalues will increase in number, but not in amplitude. This is shown in the plots of Fig. 5, where the eigenvalue profile of the measurement correlation matrix for a waveform with three cisoidal components is presented for different values of SNR. The value $M = 10$ was chosen so that a suitable number of noise-related eigenvalues could also be calculated, evidencing that, by setting a suitable threshold, signal-related eigenvalues can be singled out from noise. This holds approximately up to SNR = -8 dB, which is the threshold for the maximum likelihood estimator [16].

In the low SNR case, therefore, SVD decomposition of the measurement correlation matrix allows to carry out joint support recovery for the MMV equation (9) by searching for the sparsest solution, $\mathbf{u}$, to the equation:

$$\mathbf{v}_{X(th)} = \mathbf{W}^H \mathbf{D} \mathbf{A} \mathbf{u}, \qquad (12)$$

which, compared to the approach proposed in [17], has been modified so that $\mathbf{v}_{X(th)}$ is formed as a suitable linear combination only of the columns of $\mathbf{V}_X$ whose corresponding eigenvalues are above the threshold. As the support of $\mathbf{u}$ is equal to S_a, estimates of waveform components can be obtained again by (6), using any of the measurement vectors $\mathbf{x}_i$.

5. FINAL REMARKS

Spectral estimation of multisine waveforms is an extensively studied problem. In this paper we addressed it by a CS-based approach, showing that fine-grid frequency estimates can be obtained and component amplitudes and phases reconstructed exactly when normalized component frequencies are given by l_h/N'. Referring to a finite grid may appear as a limitation compared to interpolation and parametric methods where, in
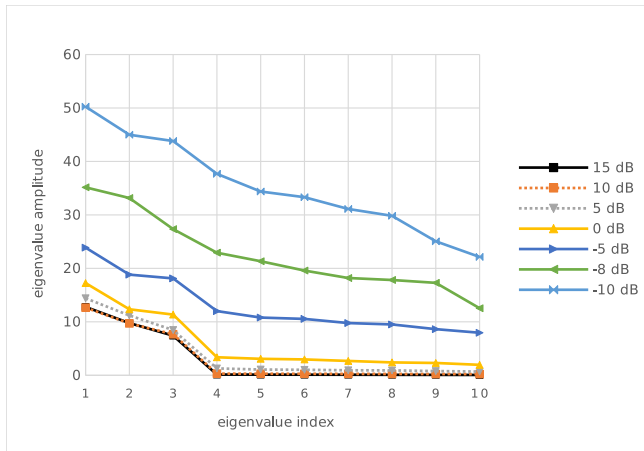
Fig. 5. eigenvalues of the measurement correlation matrix, with $M = 10$, $P = 11$.

principle, frequency can be considered a continuous variable. However, finite signal-to-noise ratio (SNR) places a lower-bound as well, which is equivalent for all practical purposes to just considering a discrete fine grid.

So far, performance of OMP in support recovery has been found adequate for applications in electrical engineering, allowing to correctly detect all components of analysed multi-sine waveforms. Investigation into CS alternatives with better noise robustness could allow to better exploit in the future the potential of some of the features discussed in the paper.

For lower SNR values, locating components lying on the finer grid requires preliminary subspace decomposition of a measurement correlation matrix. As this is obtained from M time-shifted sample sequences, each of length N, just a moderate increase in measurement time is required [18].

REFERENCES

[1] S.L. Marple, Jr., "Digital spectral analysis with applications", Prentice-Hall, Englewood Cliffs, NJ, USA, 1987.

[2] P. Stoica, R. Moses, "Spectral analysis of signals", Prentice-Hall, Upper Saddle River, NJ, USA, 2005.

[3] D. C. Rife and R. R. Boorstyn, "Multiple tone parameter estimation from discrete-time observations", *Bell Syst. Tech. J.*, vol. 55, pp. 1389-1410, 1976.

[4] V. H. Jain, W. L. Collins and D. C. Davis, "High accuracy analog measurements via interpolated FFT", *IEEE Trans. Instrum. Meas.*, vol. 28, no. 1, pp. 113-122, Jan. 1979.

[5] C. Offelli and D. Petri, "The influence of windowing on the accuracy of multifrequency signal parameter estimation", *IEEE Trans. Instrum. Meas.*, vol. 41, pp. 256-261, 1992.

[6] D. L. Donoho, "Superresolution via sparsity constraints",
SIAM J. Math. Anal., vol. 23, no. 5, pp. 1309-1331, May 1992.

[7] E. J. Candès and C. Fernandez-Granda, "Towards a mathematical theory of super-resolution", *Commun. Pure Appl. Math.*, on line 29 April 2013, http://dx.doi.org/10.1002/cpa.21455.

[8] M. F. Duarte and R. G. Baraniuk, "Spectral compressive sensing", *Appl. Comput. Harmon. Anal.*, vol. 35, no. 1, pp. 111-129, July 2013.

[9] A. Fannjiang and W. Liao, "Coherence pattern-guided compressive sensing with unresolved grids", *SIAM J. Imaging Sciences*, vol. 5, no. 1, pp. 179-202, 2012.

[10] A. Fannjiang and W. Liao, "Super-resolution by compressive sensing algorithms", Proc. IEEE 46th Asilomar Conf. Signals, Syst., Comp., Pacific Grove, CA, USA, 4-7 Nov. 2012.

[11] E. J. Candès, Y. C. Eldar, D. Needell, P. Randall, "Compressed sensing with coherent and redundant dictionaries", *Appl. Comput. Harmon. Anal.*, vol. 31, no. 1, pp. 59-73, July 2011.

[12] J.A. Tropp, A. C. Gilbert, "Signal recovery from random measurements via orthogonal matching pursuit", *IEEE Trans. Inf. Theory*, vol. 53, no. 12, pp. 4655-4666, Dec. 2007.

[13] F.J. Harris, "On the use of windows for harmonic analysis with the discrete Fourier transform", *Proc. IEEE*, vol. 66, no. 1, pp. 51-83, Jan. 1978.

[14] D. C. Rife and R. R. Boorstyn, "Single-tone parameter estimation from discerete-time observations", *IEEE Trans. Inform. Theory*, vol. 20, no.5, pp. 591-598, Sept. 1974.

[15] S.F. Cotter, B.D. Rao, K. Engan, K. Kreuz-Delgado, "Sparse solutions to linear inverse problems with multiple measurement vectors", *IEEE Trans. Signal Process.*, vol. 53, no. 7, pp. 2477-2488, Jul. 2005.

[16] B. James, B.D.O. Anderson, R.C. Williamson, "Characterization of threshold for single tone maximum likelihood frequency estimation", *IEEE Trans. Signal Process.*, vol. 43, no. 4, pp. 817-821, Apr. 1995.

[17] M. Mishali, Y. C. Eldar, "Reduce and Boost: Recovering Arbitrary Sets of Jointly Sparse Vectors", *IEEE Trans. Signal Process.*, vol. 56, no. 10, pp. 4692-4702, Oct. 2008.

[18] M. Bertocco, G. Frigo, C. Narduzzi, "On compressed sensing and super-resolution in DFT-based spectral analysis", Proceedings 19th IMEKO TC-4 Symposium and 17th IWADC Workshop *Advances in Instrumentation and Sensors Interoperability*, July 18-19, 2013, Barcelona, Spain.